Earth Moon Planets (2014) 112:15–31
DOI 10.1007/s11038-014-9435-9

# Three Peaks of 2011 Draconid Activity Including that Connected with Pre-1900 Material

**Pavel Koten · Jeremie Vaubaillon · Juraj Tóth · Anastasios Margonis · František Ďuriš**

Received: 4 September 2013 / Accepted: 11 April 2014 / Published online: 23 May 2014


**Abstract** A Draconid meteor shower outburst was observed from on board two scientific aircraft deployed above Northern Europe on 8th October 2011. The activity profile was measured using a set of photographic and video cameras. The main peak of the activity occurred around 20:15 ± 0:0.5 UT which is consistent with the model prediction as well as with the IMO network visual observations. The corrected hourly rates reached a value of almost 350. The brighter meteors peaked about 15–20 min earlier than the dimmer ones. This difference can be explained by different directions of the ejection of the meteoroids from the parent comet. One of the instruments was even able to detect meteors connected with the material ejected from the parent comet before 1900 and thus confirmed the prediction of the model, although it was based on uncertain pre-1900 cometary data. Another small peak of the activity, which was caused by material ejected during the 1926 perihelion passage of the parent comet, was detected around 21:10 UT. The mass distribution index determined using the narrow field-of-view video camera was 2.0 ± 0.1. This work shows that the observation of meteor outbursts can constrain the orbital elements, outgassing activity and existence of jets at the surface of a comet.

**Keywords** Meteors · Meteor showers · Draconids

P. Koten (✉)
Astronomical Institute of Academy of Sciences, Ondřejov Observatory, 251 65 Ondřejov, Czech Republic
e-mail: koten@asu.cas.cz

J. Vaubaillon
Institut de Mécanique Céleste et de Calcul des Éphémérides - Observatoire de Paris, 77 Avenue Denfert-Rochereau, 75014 Paris, France

J. Tóth · F. Ďuriš
Faculty of Mathematics, Physics, and Informatics, Comenius University, Mlynská dolina 842 48, Bratislava, Slovakia

A. Margonis
Department of Geodesy and Geoinformation Science, Technical University of Berlin, Berlin, Germany

## 1 Introduction

The Draconid meteor shower is one of the most interesting meteor showers ever. It occurs every year around 8th October. Although its activity is usually very low—only few meteors per hour—it sometimes produces outbursts or even big meteor storms. The parent body of this meteor shower is comet 21P/Giacobini-Zinner with an orbital period of 6.6 year.

A spectacular storm occurred in 1933 as a big surprise. Despite of 68 % illuminated rising Moon the ZHR (Zenith Hourly Rate) reached level of 10,000 meteors per hour (Jenniskens 1995). Another storm was observed in 1946 even under a full Moon. Rate was around 12,000 meteors per hour (Jenniskens 1995). Dust trails from 1900 and 1907 perihelion passages of the parent comet were responsible for both storms (Vaubaillon et al. 2011). Another peak appeared in 1952 but it was a daytime event observed by radar only (Jenniskens 1995). The shower almost reached the storm level again in 1985 (Koseki 1990). Another outburst happened over Japan in 1998 when rates reached ZHR = $720 \pm 20$. It was found that the profile of this outburst actually consists of two components with ZHR 300 and 500 (Jenniskens 2006).

The parent comet returned to the perihelion again in 2005. According to the models any strong activity was not expected. Nevertheless the CMOR radar detected significant activity above the sporadic level on 8th October. Mainly faint meteors contributed to this activity. The equivalent hourly binned ZHR was higher than 150 (Campbell-Brown et al. 2006). Double station video observation of the descending branch of the activity curve was carried out in the Czech Republic (Koten et al. 2007).

Vaubaillon et al. (2011) predicted another strong Draconid event for 8th October 2011. The model resulted into two peaks of the shower. The first one originated from older particles ejected from the comet before 1900. Intensity and timing of this encounter was highly uncertain since the orbit of the comet as well as its photometry was unknown before 1900. The encounters with individual trails were predicted to occur between 16 and 19 UT.

On the other hand the second more important peak was associated with the same material, which caused significant events in 1933 and 1946. Therefore the prediction was supposed to be very confident. The peak connected with the 1900 material was predicted at 20:01 UT. A very high level of activity was expected, although no storm.

In this paper we investigate the activity of the Draconid meteor shower as was recorded by the cameras onboard the DLR Falcon and Safire aircrafts deployed above the Northern Europe within the DRAMAC (DRAconid Multi-instrument Aircraft Campaign) airborne mission.

## 2 Observations, Instrumentation, Data Processing

The reported data are based on the observations, which were carried out from on board the DLR Falcon (registration D-CMET) and French SAFIRE Falcon (registration F-GBTM) aircrafts. Both aircrafts were deployed in formation suitable for the double station experiment above the Northern Europe and Atlantic Ocean. The DLR plane took-off from the Kiruna airport in Sweden at 18:50 UT followed by French plane 10 min later. Both planes were flying to the west for about 2 h in a serial pattern separated by a gap of 100 km. The formation was rearranged into parallel pattern for the return flight with the separation of about 110 km. The flight path and additional details on this mission are given in Vaubaillon (2014).

Since we were not granted a sufficient number of flying hours for DLR aircraft to cover both intervals of the activity, the airborne observation was focused on the second peak, for which the prediction was more confident. Nevertheless, due to kindness of the Kiruna airport personnel and DLR Falcon crew we were able to observe the first peak of the activity from the ground. The observations were carried out through the windows of the plane using both narrow field-of-view and all-sky cameras directly from the airport ramp ($\lambda = 20°19.6'$; $\delta = 67°49.3'$, altitude 494 m). The second aircraft was in the air even during the first predicted peak of the activity and the observations were carried out while flying.

There were six instruments placed onboard the DLR Falcon aircraft. Two of them were used for the activity rate measurements. One of them was an analogue narrow field-of-view video camera consisting of an Arsat 1.4/50 mm lens, a second-generation image intensifier Mullard XX1332 and an S-VHS Panasonic commercial camcorder. In this configuration the camera provides a 42° diameter field-of-view (FOV). The meteor limiting magnitude is about $+5.5^m$. The data were recorded on mini S-VHS tapes by the video camera. The frame rate was 25 images per second. The camera was provided by the Ondřejov observatory group. The second instrument was the all-sky intensified digital camera system AMOS (Automatic Meteor Orbit System) provided by the Comenius University team. FOV of this camera is 180° wide and 140° high, time resolution 15 frames per second and meteor limiting magnitude about $+3^m$. This video system is based also on the Mullard XX1332 image intensifier and Canon fish eye 2.8/15 mm lens. The data is recorded directly into the computer.

We use also the data recorded by SPOSH (Smart Panoramic Optical Sensor Head) camera (Oberst et al. 2011) deployed on the board of the SAFIRE aircraft. The camera optics consists of 10 lenses with effective focal length of 7 mm. It is equipped with CCD sensor and provides a field-of-view of 120° × 120°. With 1s exposure time the meteor limiting magnitude is about $+4.5^m$.

The tapes recorded by the narrow FOV camera were searched manually several times. Times of the occurrence of the meteors recorded by other cameras onboard both planes were used for the detection of additional meteors. Altogether 200 meteors were found. Approximately 90 % of them were identified as potential Draconid candidates. All of them were digitalized and measured using semi-automatic software MetPho (Koten 2002). Since the single station data are not sufficient for the atmospheric trajectory and heliocentric orbit calculation, those were calculated on the assumption that the meteors are Draconids. If the backward prolonged meteor path in the atmosphere passed the Draconid radiant by less than five degrees, the meteor was considered as the Draconid shower member. Such approach does not provide very precise atmospheric data—estimated error in height could be up to 5 km—but for the purpose of the activity profile determination it is sufficient. The photometric mass of the meteor was calculated from the meteor light curve (Ceplecha 1988). For the double station meteors, i.e. meteors recorded from both aircrafts, the process was more straightforward. The trajectories and orbits were calculated using standard procedures for the double station meteors (Borovička 1990), although small correction on the aircraft movement was applied. The aircraft velocity vector was subtracted from the meteor velocity.

The processing of the all-sky data was slightly different. Original AMOS cameras are used within Slovak Meteor Network on the stable ground stations (Tóth et al. 2012a). The same camera with the spatial resolution 1,280 × 960 and time resolution 15 frames per second was deployed onboard of the DLR Falcon. All the data were saved into 2 min long AVI files. The records were searched manually and then short sequences with the meteors

were produced. UFOAnalyser software (SonotaCo 2009) was used for the astrometric reduction of the data with the standard deviation of 0.05°. The limiting magnitude for the AMOS camera on board was about +3.5. The Draconid shower membership was deduced using the prolonged meteor path.

Due to the constantly moving camera, the meteors were identified in the SPOSH images by visual inspection. For the astrometric position of the meteor a custom-made software was used which extracts the points of the meteor trail and computes their position with respect to the stars in the image. For the orbit determination, a hybrid solution between different camera systems was successfully implemented after modifying the code in order to produce the same output data.

## 3 Activity Profile

### 3.1 Main Peak of Activity

Let start with the narrow FOV camera data. This camera recorded about 180 Draconid meteors within 2:45 h of recording. The observation started at 19:12 UT and ended at 22:30 UT. There was a gap between 20:45 and 21:07 UT, when the plane made a turn and the cameras were moved on the other side of the plane. To construct the activity profile curve, we calculate the numbers of meteors in 10 min intervals. We tried different intervals and a length of 10 min provides satisfactory time resolution with still quite smooth activity curve. For the middle of each interval we read the positional data of the plane and then calculated the zenith distance of the meteor shower radiant. Such knowledge is used for the correction of the number of meteors since the zenith distance of the radiant influences this number. The correction is calculated according to the equation

$$cN = N/cos(z) \tag{1}$$

where $N$ is the number of meteors in interval, $z$ is the zenith distance of the radiant and $cN$ is corrected number of meteors (Jenniskens 1994).

Using the corrected number of meteors we calculate the corrected hourly rate of meteors:

$$cHR = cN/T_{eff} \tag{2}$$

with $T_{eff} = 10$ min in this case.

To avoid confusion with zenith hourly rate (ZHR) usually used for visual observations, we call this quantity corrected instrumental hourly rate (cHR). The statistical error of cHR is then computed by equation

$$\Delta cHR = cHR/\sqrt{N} \tag{3}$$

The activity profile for the narrow FOV video camera is given in Fig. 1. We can see strong activity between 19:30 and 20:30 UT. After this time the activity dropped significantly and was very low for the rest of the mission. Aurora disturbances after 20:30 UT surely contribute to this drop of number of meteors but it cannot be the only reason for it. Still even faint meteors were seen on the records during this observational period. The activity decreased after 20:30 UT. There is a gap in the observation caused by the reconfiguration of the experiment when the planes turned for the return flight.

The activity curve shows that the peak occurred at $20:15 \pm 0:05$ UT, which corresponds to solar longitude $\lambda_0 = 195.039^o$. The corrected instrumental hourly rate reached value cHR $= 212 \pm 38$ at maximum.

Figure 1 also shows the comparison with the results of visual observations by International Meteor Organization (IMO) network. The data are available on www.imo.net. Altogether 128 observers from 28 countries contributed this IMO page. The total number of reported Draconid meteors is 6,948. According to the visual observations the maximum occurred at 20:12 UT ($\lambda_0 = 195.037°$) with ZHR $= 306 \pm 15$. This result is in very good agreement with the narrow FOV camera data.

For the all-sky camera the processing was slightly different. This camera recorded a higher number of Draconid meteors. Therefore we decided to bin meteors in 6 min long intervals. Moreover the intervals are overlapping by 3 min. Thus we derive the meteor numbers for each 3 min. The all-sky camera experienced several blackouts due to technical problems resulting in periods without any meteor detection. We corrected the number of meteors in each interval affected by blackout. The applied correction is proportional to the fraction of 6 min interval, when the camera did not record. For example if the camera recorded 25 meteors per 6 min and was 27 s out of power, the corrected number of meteors is $25 * \frac{360}{360-27} = 27$. Unfortunately, there was long blackout between 20:12 and 20:28 UT. Although short part of the intervals at beginning and end of this period were covered by the camera, the required corrections would have been substantial and therefore we exclude these data points from the analysis. When the initial numbers of meteors were corrected for short camera blackouts, the calculation of zenith hourly rate was done in the same way as for the narrow FOV camera.

The SPOSH camera data were processed in similar way as in the case of the narrow FOV camera. Again, the meteors were binned into 10 min intervals and a correction for the zenith distance of the radiant was performed.

The results are given in Fig. 2, which is providing the comparison of all three cameras as well as of the visual observations by IMO.

The explanation of the all-sky camera results is more complicate. The first peak of activity is seen at 19:54 UT ($\lambda_0 = 195.024°$) with cHR $= 338 \pm 62$. Then cHR slightly decreases but is still above 300. There is one interval dip at 20:06 UT but the activity seems to increase again to $330 \pm 1$ at 20:09 UT. The dip may be just the fluctuation, because it is detected only in one interval. Data for the next few intervals are not available due to blackout of the camera. Therefore we cannot say whether also the all-sky camera recorded the maximum of the activity detected by visual observers and narrow FOV camera. Nevertheless we can see that the all-sky camera recorded a much broader peak of the activity than other cameras. Since the all-sky camera detects rather brighter meteors in comparison with narrow FOV camera, it could suggest that the maximum of brighter meteors (i.e. bigger meteoroids) occurred 15–20 min earlier than the maximum of fainter meteors (i.e. smaller meteoroids). Moreover, the confirmation of the above statements come from the same all-sky cameras operated from the ground in Bettolla (Italy) with the highest activity in the interval 20:03–20:12 UT and the peak at $20:09 \pm 0:03$ UT (see Tóth et al. 2012b).

The SPOSH data shows two peaks around 20 UT. The first one occurred at 19:55 UT and is consistent with the all-sky camera first peak. The second one occurred at 20:15 UT, what is very close to the IMO data as well as the narrow FOV camera data. Between them there is a small decrease of the activity curve. Because it is represented only by one point, it is not clear whether this drop is significant. As the meteor limiting magnitude of the

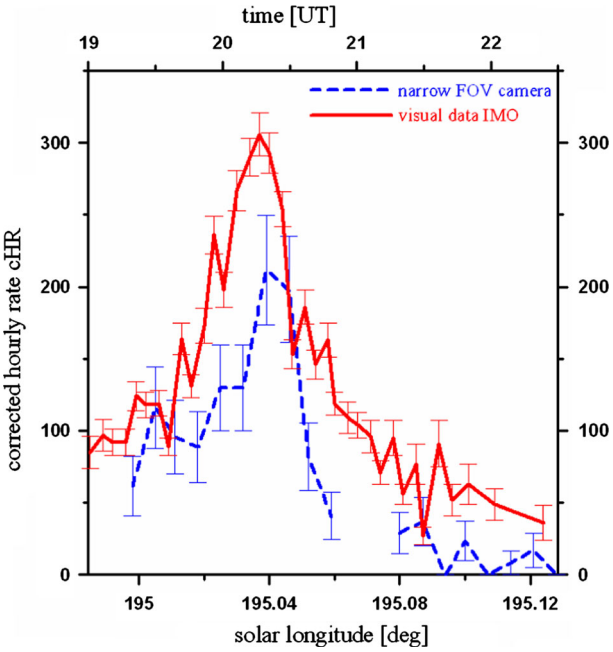


**Fig. 1** Activity profile of the Draconid meteor shower as recorded by the narrow FOV video camera aboard DLR Falcon aircraft. The gap around 21 UT represent interruption of the observation due reconfiguration of the experiment. The comparison with the visual data by IMO is also shown

SPOSH camera is closer to the narrow FOV camera, the results are comparable. Both cameras recorded a peak at 20:15 UT.

There is also a noticeable enhancement around 21:10 UT, which is recorded by both all-sky and SPOSH cameras. The activity increased for a short time interval almost two times. Because this increase was recorded by two cameras flying in two distant aircrafts, we can exclude that this is a random event. Moreover the short increase of the activity at the same time was observed also by the all-sky camera deployed in Italy (Tóth et al. 2012b). Thus we can conclude that this enhancement was a real event, which was probably caused by a small and high density region within the meteoroid stream. The modelling shows that this small peak of the activity may be associated with a material released from the parent comet in 1926.

### 3.2 Activity of Older Filaments

As mentioned at the beginning of the paper, some activity was expected also from the pre-1900 filaments, although the rate and timing was highly uncertain. Therefore we carried out single station observations with both cameras directly from the Kiruna airport ground. The narrow FOV camera was in operation from 17:10 to 18:24 UT. The conditions were far from perfect due to the proximity of Kiruna city as well as a very bright Moon. Nevertheless the cameras were still able to detect some Draconid meteors. On the other hand the SAFIRE Falcon was scheduled to cover even the first peak from the air. Therefore the SPOSH camera observations were done from on board this aircraft. Because the aircraft

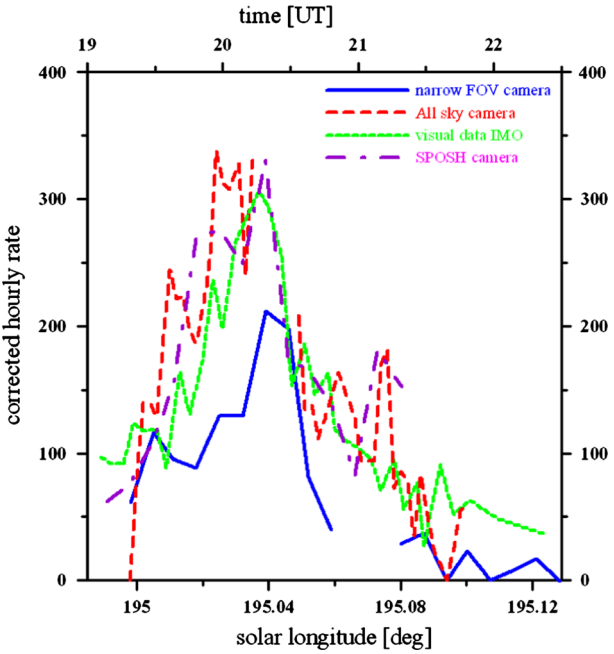


**Fig. 2** Comparison of activity profiles recorded by narrow field-of-view (*solid blue line*), all-sky camera (*dashed red line*) and SPOSH camera (*dash-dotted violet line*) as well as the visual observation results by IMO (*dotted green line*). The *error bars* are not included, because the clarity of the plot would suffer

was flying to the east, the cameras on its board were able to start the observations earlier than the cameras at the Kiruna airport.

The results of this short observational period are summarized in Fig. 3, where the corrected hourly rates (cHR) are shows. The narrow FOV camera recorded altogether 12 meteors, only one of them was not member of Draconid shower. The number of Draconids recorded by the all-sky camera is 15 and by the SPOSH camera 46. The different numbers clearly illustrate the absolutely different observation conditions between Kiruna airport and SAFIRE aircraft.

The number of the observed meteors is rather small, but the figure clearly shows that some level of Draconid activity indeed occurred during this period in a statistically significant proportion. The majority of the Draconid meteors were recorded between 17:00 a 18:00 with the peak around 17:30. Because the number of Draconid meteors is usually very low during the years of "ordinary" activity with ZHR $\sim 1$ (Jenniskens 2006), even small numbers are significant.

A question arises whether this activity represents the scattered material of the trails ejected from the parent comet before 1900 or the cameras already recorded the meteors belonging to the main peak observed later that night. A detailed look at the activity profile constructed from all the data recorded by the all-sky camera (including above mentioned ground based data) tells us more. Figure 4 shows the corrected instrumental hourly rate expressed in logarithm scale and exponential fits to both ascending and descending branches of the activity profile. We found the slopes of these exponential fits to be $B_+ = 16 \pm 1$ for ascending branch and $B_- = -17 \pm 2$ for descending one. Jenniskens (1995)

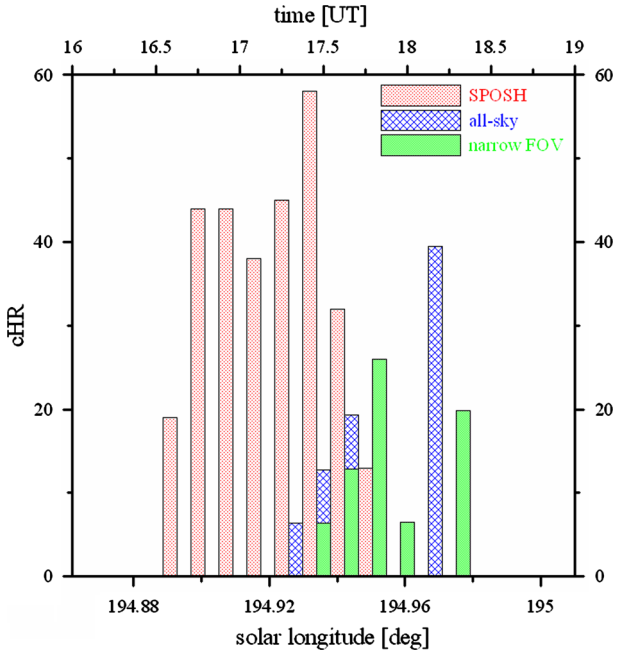


**Fig. 3** Activity of the Draconid shower during the period of the first expected peak as recorded by three cameras observations by the narrow FOV and all-sky cameras were carried out from the Kiruna airport, while the SPOSH cameras was flying on board of SAFIRE aircraft

analysed the Draconid profiles from 1933, 1946, 1952, and 1985 and pointed out that there was no significant difference in the slopes of ascending and descending branches. From this point of view it seems that the activity observed between 17:30 and 18:00 was already connected with the main peak of the meteor shower. Assuming $B = B_+ = B_-$, (Jenniskens 1995) found $B = 24 \pm 3, B = 17 \pm 2, B = 25 \pm 3$, and$B = 13 \pm 2$ for 1933, 1946, 1952, and 1985 returns. From this point of view the value B = 17 or 18 are found for the 2011 outburst are comparable. Also ground-based data from the observation campaign in Italy shows the symmetrical activity profile (Tóth et al. 2012b).

On the other hand the SPOSH camera flying on board of a SAFIRE aircraft recorded even earlier activity at the period when the cameras on the ground still could not start the observation due to dusk. This activity was noticeably higher than the counts of the meteors taken from the ground. The difference is so high that it cannot be explained only by poor observational conditions at the airport. Moreover data from the SPOSH camera do not fit the symmetrical profile of the main peak as discussed in previous paragraph. Trying to connect this early peak with the later activity we receive the ascending branch $B_+ = 6$, what is significantly lower than the values calculated for the main peak of the activity. Also as we can see from Fig. 4, later SPOSH data follows the same ascending branch of the main activity peak as the all-sky camera data. The early activity peaks around 17:20 UT when the Earth should encounter some of the trails ejected from the parent comet before 1900 (Vaubaillon et al. 2011). Thus we can conclude that the SPOSH camera indeed recorded an encounter with older material released from the comet before 1900 as was predicted. From this point of view it cannot be decided whether the Kiruna airport ground

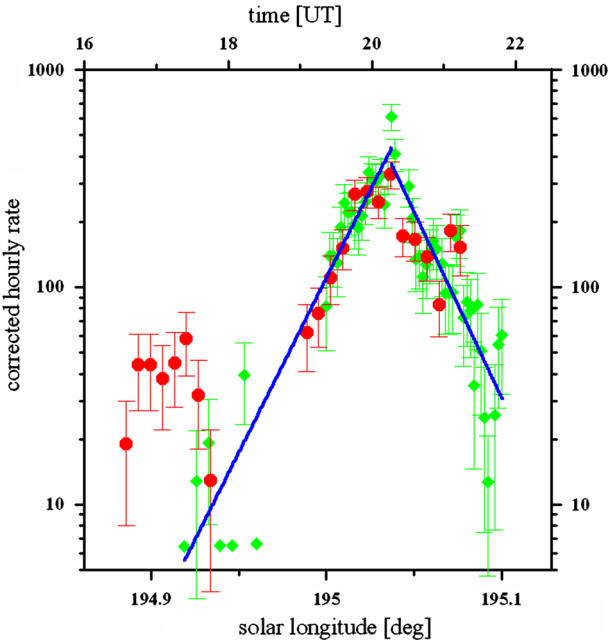


**Fig. 4** Profile of Draconid outburst activity in logarithm scale based on all the data recorded by the all-sky and SPOSH cameras. *Blue lines* show exponential fits on the all-sky camera data for ascending and descending branches. The figure shows that the profile is more symmetrical when the ground based data are included. *Red circles* represent data recorded by SPOSH camera. The first peak of activity around 17:20 UT is clearly visible

based observations cover the end of this earlier activity or the beginning of the main peak. It was probably the mix of both peaks.

## 4 Mass Distribution Index of Meteors

The mass distribution index of meteors can provide us with information on how the masses of meteoroids are distributed in the stream. If the index value is equal to 2 then there is not an excess of bigger or smaller meteoroids within the stream. If the stream predominantly consists of bigger meteoroids, the index is smaller that 2. An index greater than 2 means, that the majority of particles in the stream are small ones. The mass distribution index is usually computed using the form

$$dN = Cm^{-s}dm \tag{4}$$

where $dN$ is the number of meteors with masses between $m$ and $m + dm$ and $C$ is a constant (Ceplecha et al. 1998). We determine the slope of the plot of the logarithm of the cumulative number of meteors as a function of the logarithm of the photometric mass. If the slope is $k$ then the mass distribution index $s = 1 - k$.

For each meteor observed by the narrow FOV video camera we directly computed the photometric mass $m_p$ using the meteor light curve (Ceplecha et al. 1998). We can use about 150 Draconid meteors with a complete light curve. Figure 5 shows the results. For

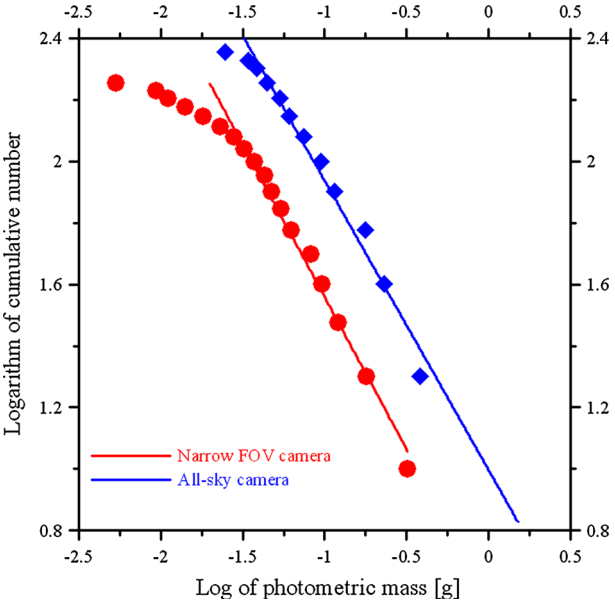


**Fig. 5** Mass distribution index for the Draconid meteors observed by both the narrow field-of-view video camera and the all-sky camera. The *solid lines* represent fits for linear part of the plot, which is used for the determination of the mass distribution index

determination of the mass distribution index we use only the linear part of this distribution. Toward small meteoroids (faint meteors) the plot becomes non-linear because the camera does not record all the faint meteors. The calculated mass distribution index $s = 2.0 \pm 0.1$. This is a reasonable value, which is comparable to values reported from previous Draconid meteor shower measurements. Campbell-Brown et al. (2006) reported $s = 2.0 \pm 0.1$ for the 2005 outburst. Koten et al. (2007) found $s = 1.87 \pm 0.15$ for the same shower. Watanabe et al. (1999) derived $s = 1.81 \pm 0.36$ for the 1998 Draconid outburst using the HDTV technique. From this point of view it seems that the 2011 Draconid meteor shower had a usual distribution of particles in the stream. The results obtained for the all-sky camera are also included in Fig. 5. We find a mass distribution index $s = 1.95 \pm 0.10$, what is similar to the narrow FOV camera.

The all-sky camera has significantly wider field-of-view than the narrow FOV camera but is less sensitive to fainter meteors. Whereas the narrow FOV camera is able to detect meteors up to +5.5 magnitudes, the limit for the all-sky camera is around +3.0 m. As was shown in the previous section, the maximum of activity as recorded by the all-sky camera started about 15–20 min earlier. Therefore we suspect that the larger meteoroids in the stream, producing brighter meteors in the sky, arrived 15–20 min earlier than smaller meteoroids producing fainter meteors.

### 4.1 Time Evolution of Mass Distribution Index

To investigate this suspicion in more details, we analyze the time evolution of the mass distribution index based on the meteors recorded by the narrow FOV camera only. This approach provides us with consistent data, which are not influenced by different sensitivity of different cameras.

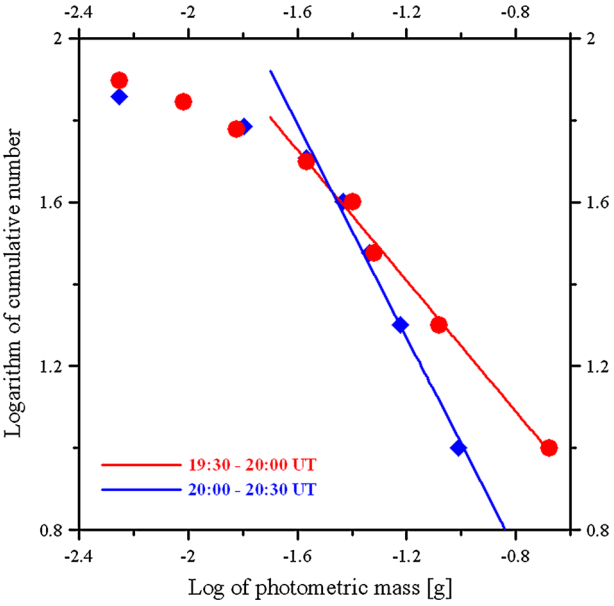


**Fig. 6** Distribution of the photometric masses for meteors recorded in two different intervals

**Table 1** The mass distribution index for different time intervals as recorded by the narrow FOV camera

| Interval | Number of meteors | Mass distribution index |
|---|---|---|
| 19:30–20:00 | 79 | 1.84 ± 0.13 |
| 19:45–20:15 | 59 | 1.93 ± 0.10 |
| 20:00–20:30 | 72 | 2.30 ± 0.06 |

We take into account three 30 min time intervals between 19:30 and 20:30 UT. The centres of the intervals are 19:45, 20:00 and 20:15 UT, meaning that intervals are overlapped by 15 min to each other. We calculate the mass distribution index from all meteors belonging to each interval. The results are summarized in Table 1. The statistical test shows that the values for first and last intervals are really different with 95 % confidence. Even if different grouping of meteors is selected for the mass distribution index computation, the results are still very similar. Figure 6 shows the comparison of the mass distribution for two of three intervals. We can see that the mass distribution index changed significantly during the observation. It was lower than two at the beginning of the observational period, meaning that brighter meteors were more abundant. On the other hand the mass distribution index was larger than two for the last interval. The abundance of fainter meteors became more significant after 20 UT. This result supports the assumption that the maximum of bright meteors occurred earlier than the maximum of faint ones.

## 5 Analysis of 2011 Draconids Profile

In this section, we examine why the small particles had a maximum AFTER the large ones, by looking at the evolution of the 1900 trail in the solar system, as a function of the particle

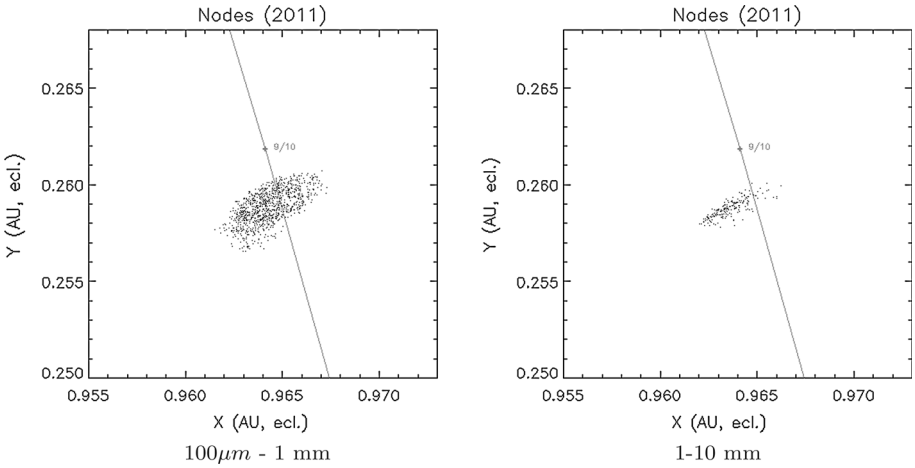


**Fig. 7** Location of the nodes of the simulated particles responsible for the 2011 Draconids, with respect to the Earth path (*line*). From these plots, we expect a broader outburst from the small particles than from the large ones

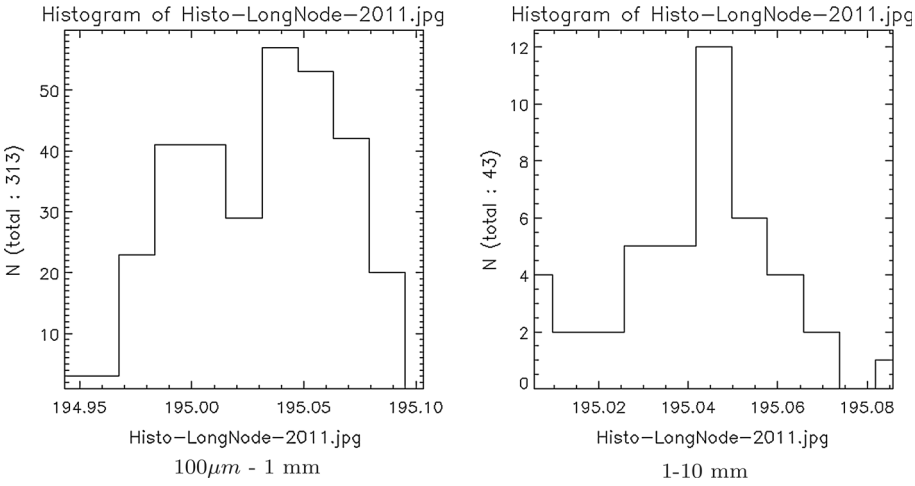


**Fig. 8** Histogram of the longitudes of the nodes for the two populations of the simulated particles responsible for the 2011 Draconids. The extent of small particles is larger than bigger ones, as expected. The profile does not look perfectly symmetrical especially for small ones

size, in the vicinity of the earth at the time of the 2011 Draconids. Therefore we plot the meteoroid ejection properties as a function of the longitude of the node for two different population of particles ([0.1;1] mm and [1;10] mm), and examine if any trend appears.

For this, we use the numerical simulation of the creation and following evolution of the Draconids meteoroid stream in the solar system, already performed by Vaubaillon et al. (2011). The method is based on Vaubaillon et al. (2005). The parent comet is numerically integrated along an arc of orbit within 3 AU from the sun. The ejection velocity of the

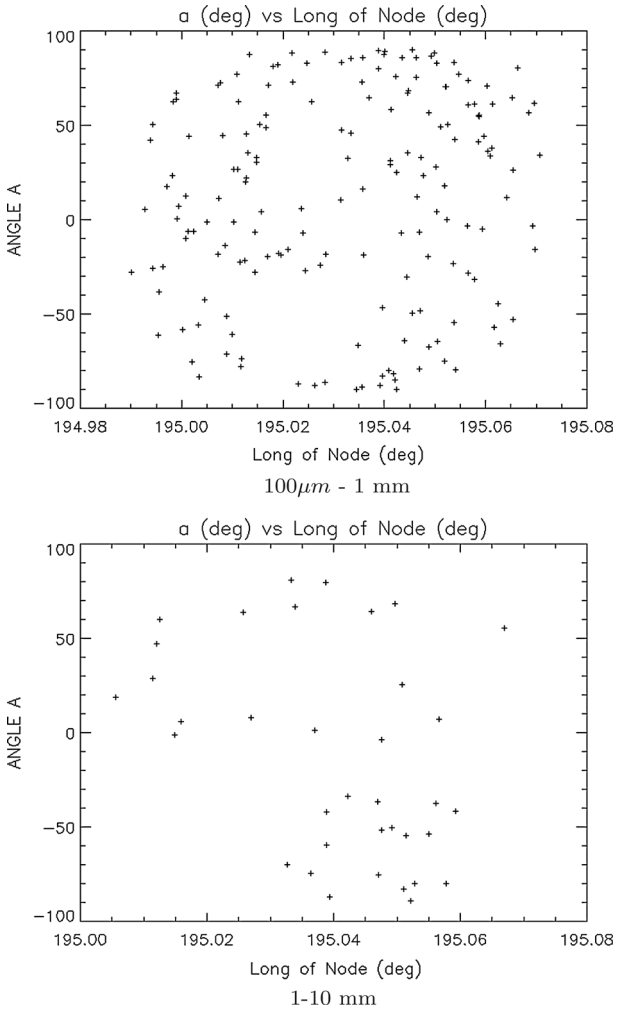


**Fig. 9** Angle of ejection of the simulated particle responsible for the 2011 Draconids in the comet orbital plane versus longitude of the node. Extreme values close to the Terminator in the morning (−90) and in the evening (+90) side) are absent for the two populations

particles is computed thanks to the Crifo and Rodionov (1997) model. The gravitation of the Sun, all the planets and the moon, as well as non-gravitational forces (radiation pressure and Poynting-Robertson drag) and first order special relativity are included. The comet orbit is taken from the JPL database. 50,000 particles per size bin are ejected at regular time interval (1 day). Three size bins are considered from 100 µm until 10 cm size. The collision with the Earth is defined by a minimum distance of the particle with our planet, at the time the particle reaches its node.

Figure 7 shows the location of the nodes as a function of the particle size, in the vicinity of the Earth's path. From these plots, we also plot the histogram of the longitude of the node, as a function of a particle size, in Fig. 8. The timing of the maximum for each population is in contradiction with observations: large particles are supposed to peak 5 min

after the small ones, according to these simulations, whereas observations tell us that they actually peaked 15 min earlier than the small ones.

In order to study this discrepancy, we now look at the direction of ejection all of the particles, in the comet reference frame. Figure 9 shows the distribution of the angle of ejection of the particle in the orbital plane of the comet. An angle equal to zero means that the particle was ejected directly towards the sun. In the simulation, this angle is limited to 90° at most (ejection in the sunlit hemisphere). The figure shows that there is no preferred value of the angle of ejection in the orbital plane of the comet.

Similarly, Fig. 10 shows the distribution of the angle of ejection of the particle out of the orbital plane of the comet. An angle equal to zero means that the particle was ejected in the orbital plane, and an angle equal to 90° means that it was ejected perpendicular to the orbital plane. Extreme values (close to the poles) are present for two populations.

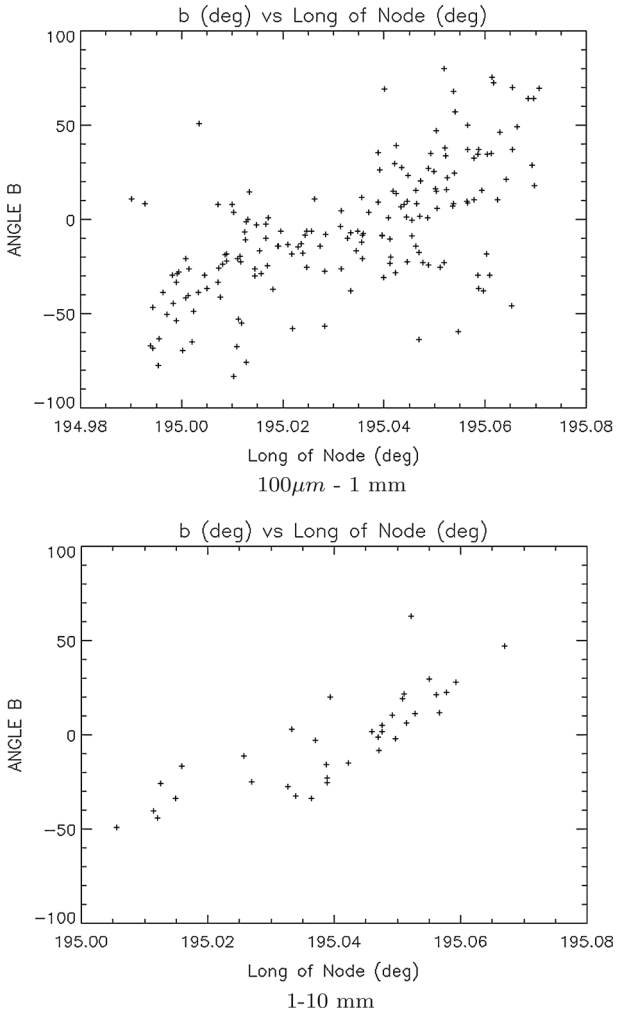


**Fig. 10** Angle of ejection of the simulated particles responsible for the 2011 Draconids outside the comet orbital plane versus longitude of the node

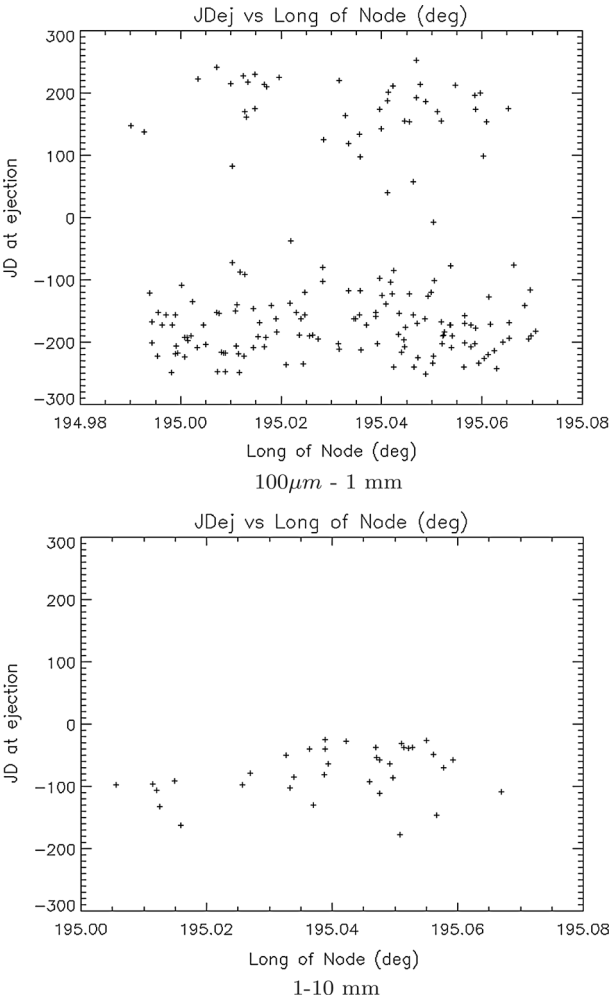


**Fig. 11** Relative time (in days ; 0 corresponds to comet perihelion passage) of the ejection of the simulated particles responsible for the 2011 Draconids, as a function of the longitude of the node

There is a clear trend for two populations. Ejections in the plane are found at the time of the maximum. The feature is more or less symmetric in angle and time for the small particles. However, it is definitely not symmetric for the large ones. Before the peak, particles are ejected under the plane, and after the peak, they are ejected above the plane. As a consequence, an early outburst can be explained by a preferred ejection direction under the orbital plane of the comet thanks to the presence of a cometary jet. A jet would indeed be more efficient at ejecting large particles than the rest of the cometary surface.

In order to test if the observed feature cannot be explained for example by preferential ejection at certain points in the orbit Fig. 11 was created. It shows the time of ejection from the comet as a function of the longitude of node for the simulated particles responsible for the 2011 Draconids. It does not show any strong evidence of a variation depending on the particle size. So we conclude that there is no dependency on the time of ejection.

## 6 Conclusions

The Draconid meteor shower outburst was successfully observed during the DRAMAC aircraft mission on 8th October 2011 and a high number of meteors was recorded using different cameras. The analyses of the activity profile shows that the main peak of Draconid activity occurred very well within the predicted time. The observation results from the video cameras are also consistent with the visual observation of IMO members. The maximum of main peak occurred at 20:15 ± 0:05 UT corresponding to a solar longitude $\lambda_0 = 195.039°$. Sensitive narrow FOV camera recorded only this maximum. On the other hand wide FOV cameras data show another peak of activity around 19:55 UT. After this peak the activity dropped for a short time and increase at 20:15 UT again. Because the wide FOV camera is less sensitive on fainter meteors, this result suggest that the brighter meteors (i.e. bigger meteoroids) peaked 15–20 min earlier than the fainter (smaller) ones.

This suspicion is confirmed by the mass distribution index computation. The data from narrow FOV video camera show that this index was changing during the observations. Its lower value before 20 UT means that brighter meteors were more abundant in the shower. An increasing value of the mass distribution index after 20 UT shows that the number of fainter meteors was higher during this period. Finally, detailed modelling of the meteoroid stream evolution confirmed that such difference can be interpreted by the presence of a cometary jet releasing more effectively larger particles than smaller ones in the direction under the orbital plane.

Assuming the symmetrical profile of the meteor activity curve, which is typical for recent Draconid outbursts and storms, we were able to separate from the main peak the particles ejected during the pre-1900 passage of the comet. Such detection is very important for the modelling of the meteoroid stream evolution, because the data regarding the comet before 1900 are very uncertain, and are only based on numerical integration based on the 1900 orbit. The activity occurred at the time predicted by the model for pre-1900 material. This shows that our current knowledge of the 1900 orbit is precise enough to infer the orbital evolution of comet 21P/Giacobini-Zinner before its discovery in 1900 and before its close approach with Jupiter in 1898.

Finally another small peak of the activity was detected around 21:10 UT. Because the cameras on board both aircrafts detected this small peak, it is not just a random hump on the activity curve. The modelling shows that this short peak is most likely associated with the material released during 1926 perihelion passage of the comet.

**Acknowledgments** Pavel Koten work was supported by the Grant Agency of the Czech Republic, grant no. 205/09/1302, by the project RVO:67985815 and by the Czech-France bilateral project 7AMB13FR006. Jeremie Vaubaillon thanks to CSAA, PNP, City of Paris and IMCEE for their support. Juraj Toth was supported by the grant APVV-0516-10. The simulations are run on a IBM CGI supercomputer (Jade) at CINES (France). The flight of the DLR Falcon aircraft was supported by EUFAR (FP7 EC funded project). The French aircraft was operated by the SAFIRE team. We thank ESA for making their SPOSH camera available for the campaign. We would like to express our gratitude to the crews of both aircrafts as well as to Kiruna airport ground staff.

## References

J. Borovička, The comparison of two methods of determining meteor trajectories from photographs. Bull. Astron. Inst. Czechoslov. **41**, 391–396 (1990)

M.D. Campbell-Brown, J. Vaubaillon, P. Brown, R. Weryk, R. Arlt, The 2005 Draconid outburst. Astron. Astrophys. **541**, 339–344 (2006)

Z. Ceplecha, Earth's influx of different populations of sporadic meteoroids from photographic and television data. Bull. Astron. Inst. Czechoslov. **39**, 221–236 (1988)
Z. Ceplecha, J. Borovička, W.G. Elford, D.O. ReVelle, R.L. Hawkes, V. Porubčan, M. Šimek, Meteor phenomena and bodies. Space Sci. Rev. **84**, 327–471 (1998)
J.F. Crifo, A.V. Rodionov, The dependence of the circumnuclear coma structure on the properties of the nucleus. Icarus **127**, 319–353 (1997)
P. Jenniskens, Meteor stream activity. I. The annual streams. Astron. Astrophys. **287**, 990–1013 (1994)
P. Jenniskens, Meteor stream activity. II. Meteor outbursts. Astron. Astrophys. **295**, 206–235 (1995)
P. Jenniskens, *Meteor Showers and Their Parent Comets* (University Cambridge Press, Cambridge, 2006)
M. Koseki, Observations of the 1985 Giacobinids in Japan. Icarus **88**, 122–128 (1990)
P. Koten, Software for processing of meteor video records, Proceedings of the Asteroids, Comets, Meteors 2002 conference, ESA SP 500, Berlin, 197–200 (2002)
P. Koten, J. Borovička, P. Spurný, R. Štork, Optical observations of enhanced aktivity of the 2005 Draconid meteor shower. Astron. Astrophys. **466**, 729–735 (2007)
J. Oberst, J. Flohrer, S. Elgner, T. Maue, A. Margonis, R. Schrödter, W. Tost, M. Buhl, J. Ehrich, A. Christou, D. Koschny, The smart panoramic optical head sensor (SPOSH) a camera for observations of transient luminous events on planetary night sides. Planet Space Sci. **59**, 1–9 (2011)
SonotaCo, Ongoing meteor work. A meteor shower catalog based on video observations in 2007–2008 WGN. J. Int. Meteor. Organ. **37**, 55–62 (2009)
J. Tóth, L. Kornoš, P. Vereš, J. Šilha, D. Kalmančok, P. Zigo, J. Világi, All-sky video orbits of Lyrids 2009. Publ. Astron. Soc. Jpn. **63**, 311–314 (2012a)
J. Tóth, R. Piffl, J. Koukal, P. Zoladek, M. Wisniewski, Š. Gajdoš, F. Zanotti, D. Valeri, P. De Maria, M. Popek, S. Gorkova, J. Világi, L. Kornoš, D. Kalmančok, P. Zigo, Video observation of Draconids 2011 from Italy. WGN J. IMO **40**, 117–121 (2012b)
J. Vaubaillon, overview paper in this issue (2014)
J. Vaubaillon, F. Colas, L. Jorda, A new method to predict meteor showers. I. Description of the model. Astron. Astrophys. **439**, 751–760 (2005)
J. Vaubaillon, J. Watanabe, M. Sato, S. Horii, P. Koten, The coming 2011 Draconid meteor shower. WGN J IMO **39**, 59–63 (2011)
J. Watanabe, S. Abe, M. Takanashi, T. Hashimoto, O. Iiyama, Y. Ishibashi, K. Morishige, S. Yokogawa, HD TV observation of the strong activity of the Giacobinid Meteor Shower in 1998. Geophys. Res. Lett. **26**, 1117–1120 (1999)